Acta Crystallographica Section B
Structural Science
ISSN 0108-7681

Molecular and crystalline structures of three (*S*)-4-alkoxycarbonyl-2-azetidinones containing long alkyl side chains from synchrotron X-ray powder diffraction data

Luis E. Seijas,[a] Asiloé J. Mora,[a]* Gerzon E. Delgado,[a] Francisco López-Carrasquero,[b] María E. Báez,[b] Michela Brunelli[c]‡ and Andrew N. Fitch[c]

[a]Laboratorio de Cristalografía, Departamento de Química, Facultad de Ciencias, Universidad de Los Andes, Mérida 5101, Venezuela, [b]Laboratorio de Polímeros, Departamento de Química, Facultad de Ciencias, Universidad de Los Andes, Mérida 5101, Venezuela, and [c]European Synchrotron Radiation Facility, BP220, F-38043 Grenoble CEDEX, France

‡ Current address: ILL Institut Laue–Langevin, BP 156, 38042 Grenoble CEDEX 9, France

Correspondence e-mail: asiloe@ula.ve

Received 6 March 2009
Accepted 9 September 2009

The (*S*)-4-alkoxo-2-azetidinecarboxylic acids are optically active β-lactam derivatives of aspartic acid, which are used as precursors of carbapenem-type antibiotics and poly-β-aspartates. The crystal structures of three (*S*)-4-alkoxo-2-azetidinecarboxylic acids with alkyl chains with 10, 12 and 16 C atoms were solved using parallel tempering and refined against the X-ray powder diffraction data using the Rietveld method. The azetidinone rings in the three compounds display a pattern of asymmetrical bond distances and an almost planar conformation; these characteristics are compared with periodic solid-state, gas-phase density-functional theory (DFT) calculations and *MOGUL* average bond distances and angles from the CSD. The compounds pack along [001] as corrugated sheets separated by approximately 4.40 Å and connected by hydrogen bonds of the type N—H···O.

1. Introduction

The (*S*)-4-alkoxo-2-azetidinecarboxylic acids have a four-membered strained heterocyclic β-lactam ring, which is difficult to synthesize owing to the unfavorable enthalpies of activation (Huszthy *et al.*, 1993). These compounds are optically active β-lactam derivatives of L-aspartic acid obtained from the transesterification of (*S*)-4-benzyloxycarbonyl-2-azetidinone. These derivatives have potential interest since they can be converted into 4-acetoxy-2-azetidinones, which are the precursors of carbapenem-type antibiotics (Nagao *et al.*, 1992*a*,*b*; Nagao, Nagase, Kumagai, Kuramoto *et al.*, 1992; Nagao, Nagase, Kumagai, Matsunaga *et al.*, 1992). Furthermore, (*S*)-4-alkoxycarbonyl-2-azetidinones can be used to prepare poly-β-aspartates by anionic open-ring polymerization (Navas *et al.*, 1997; Ramírez *et al.*, 2000). These poly-β-aspartates adopt layered structures formed from 13/4 helixes, where the side aliphatic chains crystallize in an interlayered microphase perpendicular to the main helicoidal chain only when the aliphatic chain has more than eight C atoms (López-Carrasquero *et al.*, 1994). This work discusses the molecular and crystalline structures of the compounds (*S*)-4-decyloxo-2-azetidinecarboxylic acid (I), (*S*)-4-dodecyloxo-2-azetidinecarboxylic acid (II) and (*S*)-4-hexadecyloxo-2-azetidinecarboxylic acid (III), which were obtained from synchrotron X-ray powder diffraction data. The structures will be compared with solid-state, gas-phase DFT calculations and average values for bond distances and bond angles obtained with *MOGUL* (Bruno *et al.*, 2004) in structures reported in the Cambridge Structural Database (CSD; Allen, 2002).

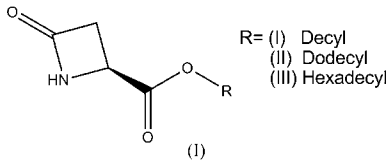

2. Experimental

2.1. Synthesis

The starting compound (*S*)-4-benzyloxycarbonyl-2-azetidinone was prepared according to Báez (2000), by a cyclization of dibenzyl L-aspartate, m.p. 412–413 K, $[\alpha]_D^{25}$: −38.7° (1.01 in CCl_3H). A vigorously stirred solution of (*S*)-4-benzyloxycarbonyl-2-azetidinone (10 mmol) and titanium(IV)tetrabutoxide (0.3 mmol) in the corresponding alcohol was heated for 2–4 h depending on the alcohol of choice. Thin layer chromatography (TLC) followed the course of the transesterification; the reaction was assumed to be over when no UV absorption indicative of traces of the reactant (*S*)-4-benzyloxycarbonyl-2-azetidinone was detectable. The compounds were separated from the concentrated reaction mixture by precipitation and finally purified by repeated crystallizations. (I): m.p. 324–325 K; $[\alpha]_D^{25}$: −25.7° (1 g dl^{-1} in CCl_3H); NMR ^1H (in CCl_3D): δ (p.p.m.) 6.08 (s, 1H, NH), 4.16 (m, 3H, CHNH and CO_2CH_2), 3.20 (m, 2H, CH_2CO), 1.67 (m, 2H, $CO_2CH_2CH_2$), 1.28 (s, 14H, $7CH_2CH_3$), 0.90 (t, 3H, CH_3); NMR ^{13}C (in CCl_3D): δ (p.p.m.) 171.01 (COO), 167.02 (CONH), 67.51 (OCH_2), 47.80 (CONH—CH), 43.57 (CH_2—CONH), 22.67 (CH_2), 14.12 (CH_3). (II): m.p. 339–340 K; $[\alpha]_D^{25}$: −22.4° (0.99 g dl^{-1} in CCl_3H); NMR ^1H (in CCl_3D): δ (p.p.m.) 6.20 (s, 1H, NH), 4.18 (m, 3H, CHNH and CO_2CH_2), 3.20 (m, 2H, CH_2CO), 1.66 (m, 2H, $CO_2CH_2CH_2$), 1.26 (broad band, 18H, $9CH_2$), 0.88 (t, 3H, CH_3); NMR ^{13}C (in CCl_3D): δ (p.p.m.) 171.01 (COO), 166.28 (CONH), 65.97 (OCH_2), 47.28 (CONH—CH), 43.56 (CH_2—CONH), 31.88, 29.58, 29.33, 29.18, 28.47, 25.77, 22.67 (CH_2), 14.11 (CH_3). (III): m.p. 349–350 K; $[\alpha]_D^{25}$: −19.1° (1 g dl^{-1} in CCl_3H); NMR ^1H (in CCl_3D): δ (p.p.m.) 6.20 (s, 1H, NH), 4.15 (m, 3H, CHNH and CO_2CH_2), 3.20 (m, 2H, CH_2CO), 1.67 (m, 2H, $CO_2CH_2CH_2$), 1.28 (broad band, 26H, $13CH_2$), 0.90 (t, 3H, CH_3); NMR ^{13}C (in CCl_3D): δ (p.p.m.) 171.05 (COO), 167.04 (CONH), 66.01 (OCH_2), 47.31 (CONH—CH), 43.57 (CH_2—CONH), 22.71 (CH_2), 14.15 (CH_3).

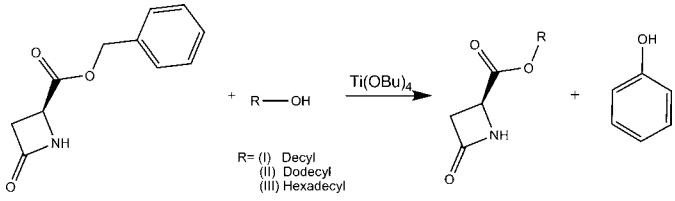

2.2. Powder data collection

The experiments were carried out at beamline ID31, ESRF (France; Fitch, 2004), selecting X-rays from an undulator source with wavelength 0.850227 (9) Å. Small quantities of each compound were lightly ground with a pestle in an agate mortar. The samples were difficult to load in the 1.0 mm diameter borosilicate glass capillaries, because the compounds crystallized as microcrystals with the shape of fibers/needles which stick to the walls of the capillary due to static electricity. For the purpose of data collection, each filled capillary was mounted on the axis of the diffractometer and spun at 1 Hz. All samples suffered from severe radiation damage; therefore, several short 3 min continuous scans were performed on different sections of each capillary. However, the comparison of the first two scans revealed strong anisotropic shifts of the Bragg reflections. Therefore, it was decided to take only the first scan for each sample in the final rebinning of the raw data into steps of $2\theta = 0.005°$. The data were carefully checked and considered of sufficient quality for the purpose of this study owing to the high brilliance of the beam used in ID31, which compensates for the counting statistics at high angles.

3. Results

3.1. Structural solutions and refinements

Powder diffraction patterns of (I), (II) and (III) were indexed with the auto-indexing program *DICVOL*04 (Boultif & Louër, 2004) in monoclinic cells with the cell parameters and figures-of-merit shown in Table 1 (refined values). Evaluation of the systematic absences showed that the three compounds crystallize in the space group $P2_1$ (No. 4) with Z = 2. The diffraction patterns of (I) and (II) showed several unindexed peaks (5 and 8). They were identified as traces (less than 3%) of the starting material (*S*)-4-benzyloxycarbonyl-2-azetidinone [tetragonal cell parameters: a = 8.3887, c = 29.634 Å; $M(8) = 82.6$, $F(8) = 87.0$] used during the synthesis of both compounds.

The parallel tempering algorithm implemented in the program *FOX* (Favre-Nicolin & Černý, 2002) was used to solve the structures. Each solution required 10 million moves. The initial models were constructed using a geometry optimization at the AM1 level with the program *GAMESS* (Schmidt *et al.*, 1993) and introduced in the form of *Z* matrices. For each molecule, all three torsion angles around the oxycarbonyl group were allowed to move, while the torsion angles of the aliphatic chains [decyl in (I), dodecyl in (II) and hexadecyl in (III)] were constrained to be 180°, hence the chain was kept planar. The atoms in the azetidinone rings were unrestrained. For each run, the program *FOX* gave several solutions with similar values for the cost functions; therefore, it was necessary to check each of the solutions to discern which one was the most reliable in terms of crystal packing and stereochemical logic. Finally, the H atoms were placed in calculated positions with restricted geometries using the command HFIX from *SHELXL* (Sheldrick, 2008). The Rietveld (1969) refinement of the structures using *GSAS* (Larson & Von Dreele, 2000) used the same criteria: the background was modeled using a Chebyschev polynomial function with 15 terms; then, a correction for diffuse scattering caused by

Table 1
Experimental details.

For all structures: monoclinic, $P2_1$, $Z = 2$. Experiments were carried out at 298 K with synchrotron radiation, $\lambda = 0.850227$ Å using a high-resolution diffractometer ID31, ESRF, Grenoble, France.

	(I)	(II)	(III)
Crystal data			
Chemical formula	$C_{14}H_{25}NO_3$	$C_{16}H_{29}NO_3$	$C_{20}H_{37}NO_3$
M_r	255.36	283.41	339.52
a, b, c (Å)	27.82406 (16), 5.35267 (4), 5.16992 (3)	31.0841 (3), 5.35782 (4), 5.21197 (5)	37.1586 (3), 5.35911 (5), 5.30974 (5)
β (°)	92.0469 (4)	94.1094 (7)	92.1693 (6)
V (Å^3)	769.48 (1)	865.786 (12)	1056.608 (16)
$M(20)$†, $F(20)$‡	131.9, 388.3	121.1, 363.2	142.1, 331.6
D_x (Mg m^{-3})	1.102	1.087	1.067
μ (mm^{-1})	0.076	0.074	0.070
Particle morphology	Needles	Needles	Needles
Color	White	White	White
Specimen shape, size (mm)	Cylinder, 40 × 1.0	Cylinder, 40 × 1.0	Cylinder, 40 × 1.0
Specimen preparation temperature (K)	298	298	298
Data collection			
Specimen mounting	Borosilicate glass capillary	Borosilicate glass capillary	Borosilicate glass capillary
Mode	Transmission	Transmission	Transmission
Scan method	Continuous	Continuous	Continuous
Illuminated area (mm)	1 × 2	1 × 2	1 × 2
Absorption correction	None	None	None
2θ (°)	$2\theta_{min} = 1.505$, $2\theta_{max} = 32.065$, $2\theta_{step} = 0.005$	$2\theta_{min} = 1.005$, $2\theta_{max} = 32.065$, $2\theta_{step} = 0.005$	$2\theta_{min} = 0.505$, $2\theta_{max} = 32.065$, $2\theta_{step} = 0.005$
Refinement			
R factors and goodness of fit	$R_p = 0.075$, $R_{wp} = 0.104$, $R_{exp} = 0.060$, $R(F^2) = 0.08634$, $\chi^2 = 3.098$	$R_p = 0.071$, $R_{wp} = 0.100$, $R_{exp} = 0.054$, $R(F^2) = 0.06302$, $\chi^2 = 3.497$	$R_p = 0.078$, $R_{wp} = 0.107$, $R_{exp} = 0.049$, $R(F^2) = 0.06998$, $\chi^2 = 4.928$
Excluded region(s)	None	1.400 to 1.435 and 4.270 to 4.280	1.725 to 1.765
Experimental points	6233	6351	6488
Profile function	CW profile function number 4	CW profile function number 4	CW profile function number 4
Preferred orientation correction	Spherical harmonic	Spherical harmonic	Spherical harmonic
No. of parameters	193	222	256
No. of restraints	122	140	185
$(\Delta/\sigma)_{max}$	0.04	0.04	0.03
$\Delta\rho_{min}$, $\Delta\rho_{max}$ (e Å^{-3})	−0.31, 0.27	−0.22, 0.20	−0.18, 0.19

† See de Wolff (1968). ‡ See Smith & Snyder (1979).

vibrational correlation was made. The peak shapes were modeled with a pseudo-Voigt function (Thompson *et al.*, 1987), which included a low-angle axial divergence correction (Finger *et al.*, 1994) and anisotropic line broadening (Stephens, 1999). Restraints were applied to bond distances and bond angles weighted to ± 0.005 Å and ± 2.0°. The azetidinone ring was restrained using the bond distances and bond angles taken from the analogous structure PELJUM (Mora *et al.*, 2006). For the aliphatic chain, the average values for the restrained bond distances and bond angles were obtained from the evaluation of 245 aliphatic chains using the program *ConQuest* (Version 1.11; Bruno *et al.*, 2002) implemented in the CSD (Version 5.29, January 2008; Allen, 2002). In the final stages of the refinement, it was necessary to apply loose planar restraints (weighted 0.2 Å) to the atoms within the azetidinone rings to avoid excessive ring distortions. Likewise, for (III) a planar restraint was applied to the 16 C aliphatic side chain (weighted 0.5 Å). The isotropic displacement factors of the atoms were refined in separate blocks; one U_{iso} for all non-H atoms of the azetidinone ring and one U_{iso} for the alkoxycarbonyl substituent. The isotropic displacement factor for all H atoms was refined as 1.2 times the U_{iso} of the parent atoms. Finally, the secondary phase corresponding to the compound (*S*)-4-benzyloxycarbonyl-2-azetidinone, which was present in (I) and (II) was extracted from the diffraction pattern by the Le Bail method (Le Bail *et al.*, 1988), which improved the overall R factors by ∼ 1%. Details of the experiments and final R values for the Rietveld refinement are summarized in Table 1.[1] The Rietveld plots are shown in Fig. 1.

3.2. DFT calculations

Periodic, solid-state calculations were performed using the *CASTEP* program implemented in *Materials Studio* (Accelrys Inc., 2001). *CASTEP* is an *ab initio* quantum-mechanical program employing density-functional theory (DFT) to simulate the properties of solids. The following execution parameters were used: GGA-PBE PAW potentials (Kresse & Joubert, 1999), SCF electronic tolerance at 2.0 exp (−6) eV per atom, an optional cut-off controlling the accuracy of the calculations set to 400 eV, a 1 × 2 × 2 k-mesh for the reci-

[1] Supplementary data for this paper are available from the IUCr electronic archives (Reference: KD5033). Services for accessing these data are described at the back of the journal.

procal space integration with a Monkhorst–Pack scheme (Monkhorst & Pack, 1976), and a Methfessel–Paxton smearing with a width of 0.2 eV for energy corrections (Methfessel & Paxton, 1989). Atomic-coordinate-only optimizations of the three compounds were performed using the experimental cell parameters and atomic positions obtained from the X-ray powder diffraction Rietveld refinement.

In order to also compare the structures with a single molecule in the gas phase, DFT quantum chemical calculations were performed in a modified molecule with the alkoxycarbonyl substituent changed to a methyloxycarbonyl group, using a Beckés three-parameter hybrid exchanged functional (Becke, 1993) and the correlation functional of Lee *et al.* (1988) with the 6-31G+(d,p) basis set. All calculations were carried out using the program *GAMESS* (Schmidt *et al.*, 1993).

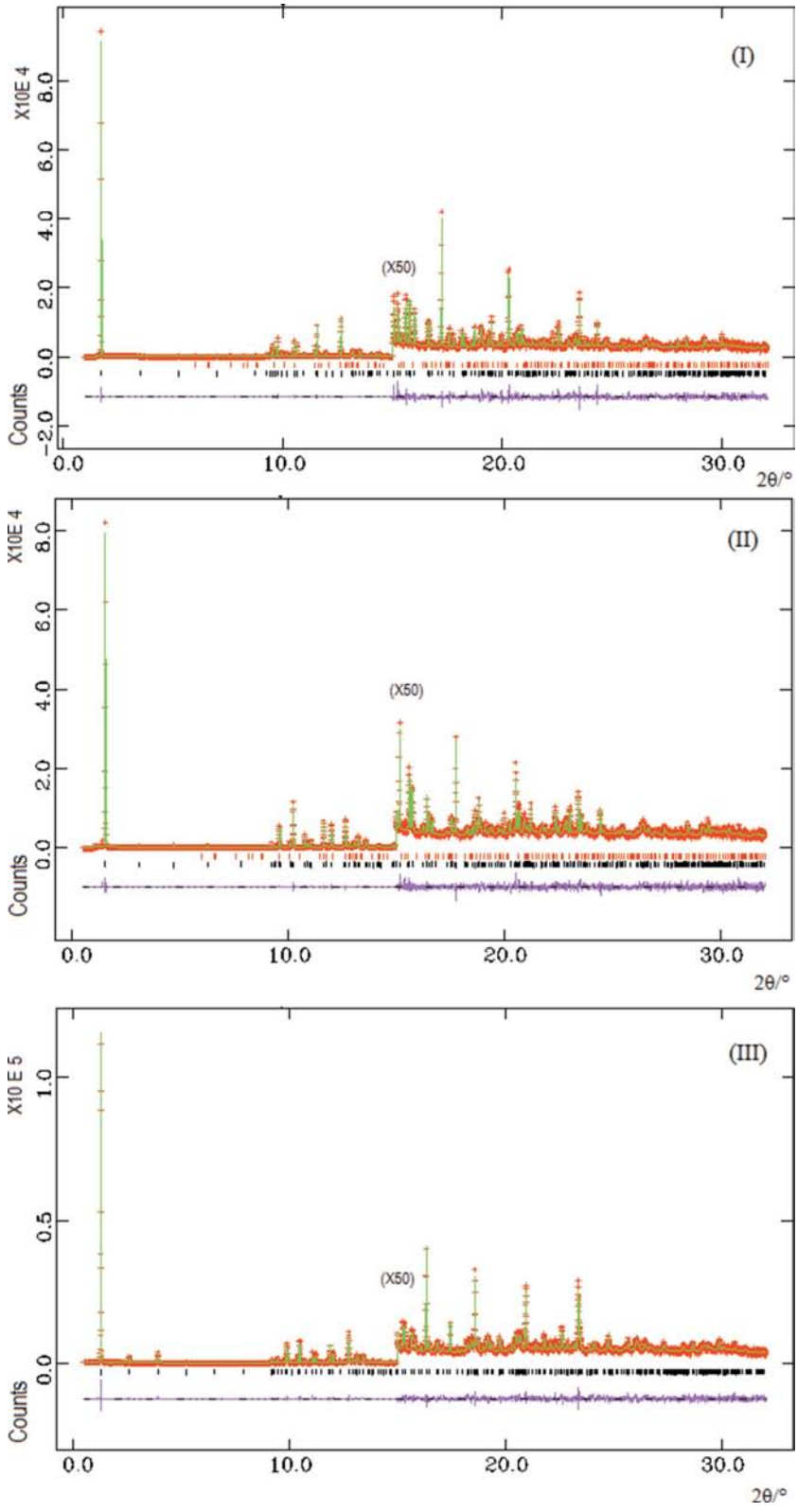

Figure 1
Final observed (points), calculated (lines) and difference profiles of the Rietveld plot for (*S*)-4-decyloxo-2-azetidinecarboxylic acid (I), (*S*)-4-dodecyloxo-2-azetidinecarboxylic acid (II) and (*S*)-4-hexadecyloxo-2-azetidinecarboxylic acid (III).

4. Discussion

Fig. 2 shows the molecular diagrams of (I), (II) and (III). Tables 2 and 3 display relevant bond distances, bond angles and torsion angles for the three compounds compared with those derived from the periodic solid-state and in-vacuum DFT theoretical calculations and averages obtained with *MOGUL* from searches based on related molecular fragments run on the CSD. The chiral environment of atom C3 and the mixed hybridization states of all the atoms within the azetidinone ring (N2 and C1 are sp^2, C3 and C4 are sp^3) make this a strained four-membered ring, asymmetrical and non-planar. However, the three rings display almost planar conformations with maximal deviations from planarity localized in C1 [0.015 (6), 0.042 (7) Å for (I) and (II)], and in N2 [0.02 (1) Å] for (III).

Bond distances in rings (I) and (II) display similar asymmetry patterns (C4—C3 > C1—C4 > N2—C3 > C1—N2), which are also seen in the in-vacuum theoretical calculations at a DFT/B3LYP level, and in nine of the ten related structures found in the CSD [PELJUM (Mora

Table 2
Selected bond distances (Å) and bond angles (°).

	(I)		(II)		(III)				(I)	(II)	(III)	(I)	(II)	(III)
	XRD	DFT†	XRD	DFT†	XRD	DFT†	*MOGUL* (mean)	DFT/B3LYP‡ (gas phase)	(XRD-DFT)	(XRD-DFT)	(XRD-DFT)	(XRD-*MOGUL*)	(*MOGUL*)	
C1—N2	1.34 (2)	1.36	1.34 (2)	1.36	1.35 (6)	1.36	1.34 (4)	1.376	−0.02	−0.02	−0.01	0.00	0.00	−0.01
N2—C3	1.477 (5)	1.46	1.477 (7)	1.47	1.38 (1)	1.46	1.47 (1)	1.462	0.02	0.01	−0.08	0.00	0.00	−0.09
C3—C4	1.546 (4)	1.51	1.543 (6)	1.51	1.52 (1)	1.52	1.55 (1)	1.568	0.04	0.03	0.01	0.00	0.01	−0.03
C4—C1	1.504 (6)	1.56	1.502 (8)	1.56	1.54 (2)	1.57	1.52 (2)	1.550	−0.06	−0.06	0.03	−0.02	−0.04	0.02
C1—O5	1.23 (1)	1.24	1.23 (1)	1.24	1.20 (5)	1.24	1.23 (2)	1.207	−0.01	−0.01	−0.04	0.00	0.00	−0.03
C3—C6	1.505 (5)	1.51	1.505 (7)	1.52	1.50 (1)	1.51	1.52 (3)	1.519	−0.01	−0.01	−0.01	−0.01	−0.01	−0.02
C6—O7	1.229 (6)	1.23	1.228 (7)	1.23	1.24 (1)	1.23	1.20 (3)	1.213	0.00	0.00	0.01	−0.03	0.03	0.04
C6—O8	1.325 (5)	1.35	1.322 (7)	1.35	1.32 (1)	1.35	1.33 (2)	1.346	−0.03	−0.03	−0.03	0.00	−0.01	−0.01
O8—C9	1.453 (5)	1.46	1.448 (7)	1.45	1.46 (1)	1.46	1.45 (3)	1.440	−0.01	0.00	0.00	0.00	0.00	0.01
C—C_{mean}	1.503 (4)	1.53	1.504 (5)	1.52	1.51 (4)	1.52	1.51 (6)		−0.03	−0.02	0.01	−0.01	−0.01	0.00
N2—C1—C4	91.3 (7)	93.3	90.6 (8)	93.2	91 (3)	93.2	92.3 (9)	90.89	−2.0	−2.6	−2.2	−1.0	−1.7	−1.3
N2—C1—O5	131.8 (5)	131.5	132.0 (7)	131.3	133 (2)	131.6	132 (1)	132.95	0.3	−1.7	1.4	−0.2	0.0	−1.2
C4—C1—O5	136.2 (1)	135.2	135.4 (1)	135.5	136 (4)	135.2	136 (1)	136.16	1.0	−0.1	0.8	0.2	−0.6	0.0
C1—N2—C3	96.6 (3)	94.7	96.9 (5)	94.6	95 (1)	95.0	95.7 (8)	96.46	1.9	2.3	0.0	0.9	1.2	0.7
N2—C3—C4	84.8 (2)	87.2	84.1 (3)	87.1	91.4 (6)	87.1	87.0 (8)	87.05	−2.4	−3.0	4.3	−2.2	−1.9	4.4
C3—C4—C1	87.4 (6)	84.7	87.7 (7)	85.1	82 (2)	84.7	86 (1)	85.53	2.4	2.6	−2.7	1.4	1.7	4.0
N2—C3—C6	112.3 (3)	117.1	113.3 (5)	111.5	110.8 (9)	116.2	115 (2)	118.74	−4.8	1.8	−5.4	−2.7	−1.7	−4.2
C4—C3—C6	113.9 (3)	113.2	114.8 (4)	118.1	114.1 (6)	114.4	115 (4)	115.64	0.7	−3.3	−0.3	−1.1	−0.2	−0.9
C3—C6—O7	123.3 (4)	123.4	124.7 (5)	125.1	124.5 (9)	123.1	124 (3)	122.67	−0.1	−0.4	1.4	−1.0	0.7	0.5
C3—C6—O8	112.9 (3)	112.2	113.1 (4)	110.3	112.8 (7)	112.2	112 (2)	112.87	0.7	2.8	0.6	0.9	1.1	0.8
O7—C6—O8	122.0 (4)	121.2	121.3 (5)	124.5	119.9 (8)	124.7	124 (2)	124.44	−1.2	−3.2	−4.8	−2.0	−2.7	4.1
C6—O8—C9	117.0 (3)	116.4	116.9 (4)	119.1	118.2 (7)	116.6	117 (4)		1.4	−2.2	1.6	0.0	−0.1	1.2
C—C—C_{mean}	113.4 (2)	114.8	113.4 (2)	114.4	113.7 (2)	113.5	115 (5)		−1.4	−1.0	0.2	−1.6	−1.6	−1.5

Computer program used: *MOGUL*1.1 (Bruno *et al.*, 2004) run on the CSD (Allen, 2002). † Solid-state calculations performed in *CASTEP* (Accelrys Inc., 2001). ‡ Gas-phase calculations performed for (*S*)-4-methyloxycarbonyl-2-azetidinone.

et al., 2006), ABADOX (Basak *et al.*, 2004), EABLEY (Robinson & Donahue, 1992), FEPNAP (Yang *et al.*, 1987), PERVIS (Tanaka *et al.*, 2006), REPLON (Bandoli *et al.*, 1995), SAZCOL (Bando *et al.*, 1989), JEFRER (Toda *et al.*, 1990) and VUJHOX (Nagao *et al.*, 1992*a*)]. On the other hand, (III) displays a different asymmetry pattern (C1—C4 > C4—C3 > N2—C3 > C1—N2), which matches the patterns observed in the remaining structure of the CSD [FEHWOE (Nagao *et al.*, 1987)].

A comparison of the structures with their periodic solid-state DFT calculations by analysis of the deviations of bond distances and bond angles show the average differences do not exceed 0.02 Å and 1.1° [largest deviations = +0.04 and −0.06 Å for (I); +0.03 and −0.06 Å for (II); +0.03 and −0.08 Å for (III). Largest deviations: +2.4 and −4.8° for (I); +2.8 and −3.3° for (II); +4.3° and −5.4 ° for (III)]. Comparing the

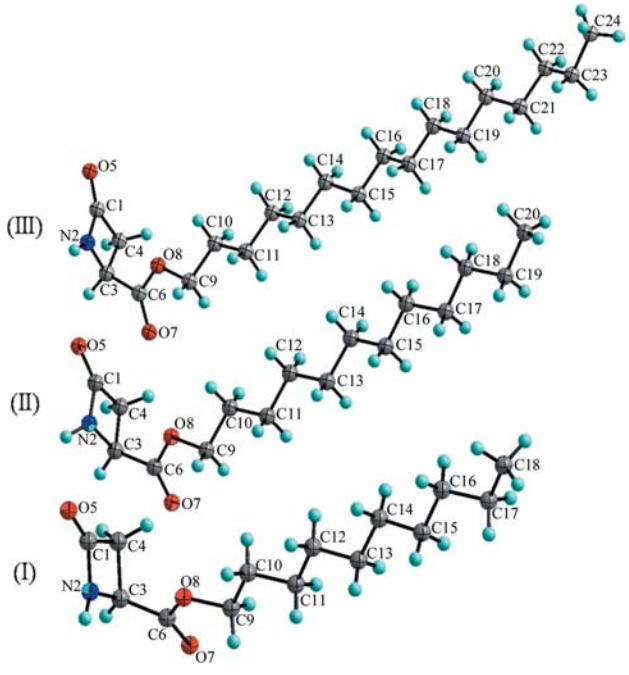

Figure 2
Molecular diagrams for (*S*)-4-decyloxo-2-azetidinecarboxylic acid (I), (*S*)-4-dodecyloxo-2-azetidinecarboxylic acid (II) and (*S*)-4-hexadecyloxo-2-azetidinecarboxylic acid (III), showing the atom-labelling scheme.

Figure 3
Molecular overlay of (*S*)-4-decyloxo-2-azetidinecarboxylic acid (I) (blue), (*S*)-4-dodecyloxo-2-azetidinecarboxylic acid (II) (yellow) and (*S*)-4-hexadecyloxo-2-azetidinecarboxylic acid (III) (red), showing a comparison of the alkyl ester orientation.

Table 3
Selected torsion angles(°).

	(I)		(II)		(III)	
	XRD	DFT	XRD	DFT	XRD	DFT
N2—C3—C6—O8	−43.6 (4)	−34.3	−41.4 (6)	−55.8	−45 (1)	−36.8
C3—C6—O8—C9	−174.4 (3)	162.9	178.7 (4)	163.7	176.2 (7)	174.5
C10—C9—O8—C6	165.9 (3)	177.6	159.5 (5)	143.6	163.4 (8)	161.9

Table 4
Hydrogen bonds (Å, °).

	D—H···A	D—H	H···A	D···A	D—H···A
(I)	N2—H21···O5^{i}	0.96 (1)	2.18 (1)	2.91 (1)	131.8 (8)
(II)	N2—H21···O5^{i}	0.96 (1)	2.20 (1)	2.91 (1)	131.2 (7)
(III)	N2—H21···O5^{i}	0.96 (2)	2.17 (3)	2.88 (1)	130 (2)

Symmetry codes: for (I) (i) $-1-x,-\frac{1}{2}+y,-1-z$; for (II) (i) $1-x,\frac{1}{2}+y,2-z$; for (III) (i) $1-x,-\frac{1}{2}+y,3-z$.

structures with the in-vacuum DFT B3LYP/6–31+G(d,p) theoretical calculations show average deviations of bond distances of 0.01 Å and bond angles 1.1° [largest deviations = +0.04 and −0.06 Å for (I); +0.03 and −0.06 Å for (II); +0.03 and −0.06 Å for (III); largest deviations: +2.4 and −4.8° for (I); +2.6 and −3.3° for (II); +4.3 and −5.4° for (III)]. Finally, the structures compared with the averages found with *MOGUL* show the following figures: average deviations of bond distances of 0.007 Å and bond angles 0.5° [largest deviations = +0.00 and −0.03 Å for (I); +0.03 and −0.04 Å for (II); +0.04 and −0.09 Å for (III); largest deviations: +1.4 and −2.7° for (I); +1.7° and −2.7° for (II); +4.4 and −4.2° for (III)]. It is noticeable that there is clearly a better agreement with the experimental average bond distances and bond angles found by *MOGUL* than with any of the theoretical DFT calculations. This might be attributed to inadequacy in the potentials used to describe the organic molecules along with the basis set truncation error (Ramachandran *et al.*, 2008).

The average torsion angles Csp^3—Csp^3—Csp^3—Csp^3 in the alkyl chains are 171, 176 and 172° for (I), (II) and (III), which indicates the chains are linear and forcing the CH_2—CH_2 bonds to arrange in the *gauche* conformation. The torsion angle C3—C6—O8—C9 (see Table 3) around the alkyl ester group varies from 174 to 178°. Fig. 3 shows how this torsion angle modifies the orientation of the chain in each of the compounds, which all tend to have the wedge-like shape.

In the solid state, each of the three compounds packs in layers along **b** (see Figs. 4, 5 and 6), with hydrophobic regions between neighboring alkyl chains and hydrophilic regions connecting neighboring azetidinone rings through a hydrogen bond of the type N2—H21···O5 [(I): (i) $-1-x,-\frac{1}{2}+y,-1-z$; (II): (i) $1-x,\frac{1}{2}+y,2-z$; (III): (i) $-1-x,-\frac{1}{2}+y,3-z$]. Relevant distances and angles for this hydrogen bond are displayed in Table 4. Molecules related by a 2_1 axis connect by hydrogen bonds to form infinite chains extending along the [010] direction. This motif is described by the graph $C(4)$ (Etter, 1990). All these interactions produce corrugated sheets piled up along the [001] direction and separated by approximately 4.40 Å. The packing efficiency was calculated using the program *PLATON* (Spek, 2009); these values in the structures are 63.8, 63.9 and 64.0%, for (I), (II) and (III), respectively.

We thank the ESRF for providing synchrotron radiation beam time (project No. CH-2490), CDCHT-ULA (grant C-1618-08-08-AA) and FONACIT (grant LAB-97000821).

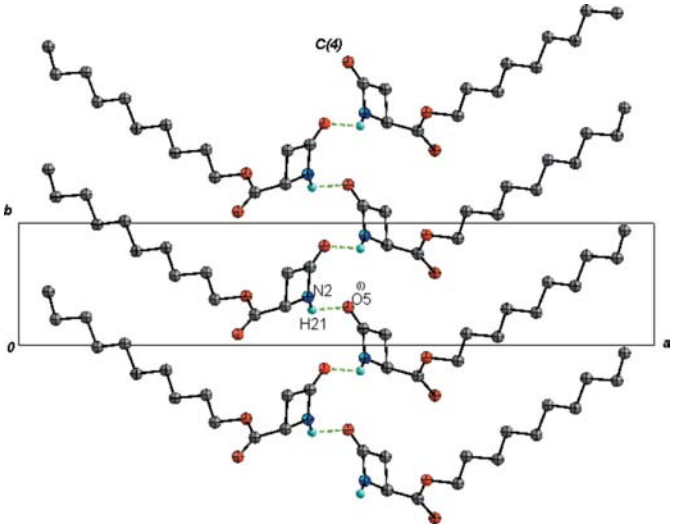

Figure 4
Extended supramolecular $C(4)$ chain constructed from hydrogen bonds N2—H21···O5 [(i) $-1-x,-\frac{1}{2}+y,-1-z$] in (*S*)-4-decyloxo-2-azetidinecarboxylic acid (I).

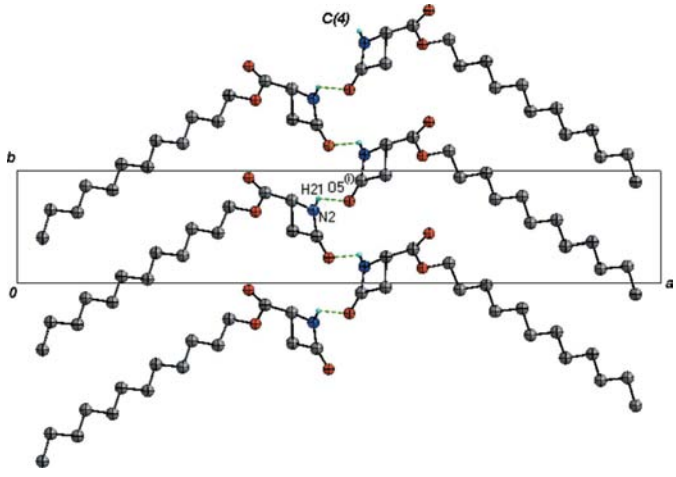

Figure 5
Extended supramolecular ribbon structure constructed from hydrogen bonds N2—H21···O5 [(i) $1-x,\frac{1}{2}+y,2-z$] in (*S*)-4-dodecyloxo-2-azetidinecarboxylic acid (II).

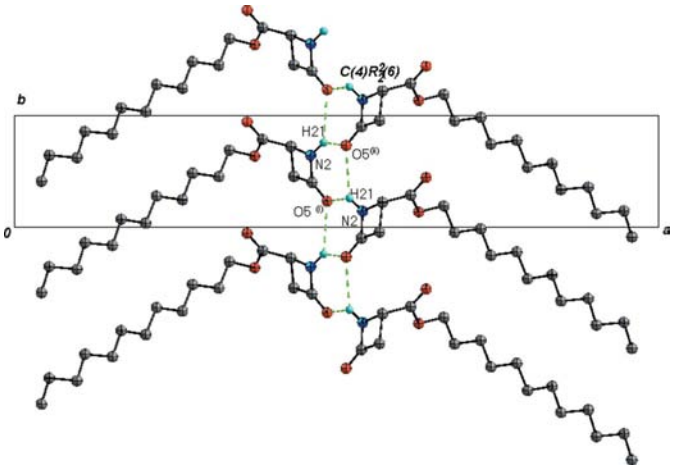

Figure 6
Extended supramolecular $C(4)$ chain constructed from the hydrogen bond N2—H21···O5 [(i) $1-x, -\frac{1}{2}+y, 3-z$] in (*S*)-4-decyloxo-2-azetidinecarboxylic acid (I).

References

Accelrys Inc. (2001). *Materials Studio*. Accelrys Inc., San Diego, California, USA.
Allen, F. H. (2002). *Acta Cryst.* B**58**, 380–388.
Báez, M. E. (2000). Thesis, Universidad de Los Andes, Venezuela.
Bando, S., Takano, T., Miyahara, K., Tanaka, R., Nakatsuka, T. & Ishiguro, M. (1989). *Acta Cryst.* C**45**, 1776–1778.
Bandoli, G., Dolmella, A., Gatto, S. & Nicolini, M. (1995). *J. Mol. Struct.* **354**, 213–225.
Basak, A., Bag, S. S., Mazumdar, P. A., Bertolasi, V. & Das, A. K. (2004). *J. Chem. Res.* pp. 318–321.
Becke, A. D. (1993). *J. Chem. Phys.* **98**, 5648–5652.
Boultif, A. & Louër, D. (2004). *J. Appl. Cryst.* **37**, 724–731.
Bruno, I. J., Cole, J. C., Edgington, P. R., Kessler, M., Macrae, C. F., McCabe, P., Pearson, J. & Taylor, R. (2002). *Acta Cryst.* B**58**, 389–397.
Bruno, I. J., Cole, J. C., Kessler, M., Luo, J., Motherwell, W. D. S., Purkis, L. H., Smith, B. R., Taylor, R., Cooper, R. I., Harris, S. E. & Open, A. G. (2004). *J. Chem. Inf. Comput. Sci.* **44**, 2133–2144.
Etter, M. C. (1990). *Acc. Chem. Res.* **23**, 120–126.
Favre-Nicolin, V. & Černý, R. (2002). *J. Appl. Cryst.* **35**, 734–743.
Finger, L. W., Cox, D. E. & Jephcoat, A. P. (1994). *J. Appl. Cryst.* **27**, 892–900.
Fitch, A. N. (2004). *Res. Natl. Inst. Stand. Technol.* **109**, 133–142.
Huszthy, P., Bradshaw, J. S., Krakowiak, K. E., Wang, T. & Dalley, N. K. (1993). *J. Heterocycl. Chem.* **30**, 1197–1207.
Kresse, G. & Joubert, D. (1999). *Phys. Rev. B*, **59**, 1758–1775.
Larson, A. C. & Von Dreele, R. B. (2000). *GSAS*. Report LAUR 86–748. Los Alamos National Laboratory, New Mexico, USA.
Le Bail, A., Duroy, H. & Fourquet, J. L. (1988). *Mater. Res. Bull.* **23**, 447–452.
Lee, C., Yang, W. & Parr, R. G. (1988). *Phys. Rev. B*, **37**, 785–789.
López-Carrasquero, F., García-Alvarez, M. & Muños-Guerra, S. (1994). *Polymer*, **35**, 4202–4510.
Methfessel, M. & Paxton, A. T. (1989). *Phys. Rev. B*, **40**, 3616–3621.
Monkhorst, H. J. & Pack, J. D. (1976). *Phys. Rev. B*, **13**, 5188–5192.
Mora, A. J., Brunelli, M., Fitch, A. N., Wright, J., Báez, M. E. & López-Carrasquero, F. (2006). *Acta Cryst.* B**62**, 606–611.
Nagao, Y., Kumagai, T., Abe, T., Ochiai, M., Taga, T., Machida, K. & Inoue, Y. (1987). *J. Chem. Soc. Chem. Commun.* pp. 602–604.
Nagao, Y., Kumagai, T., Nagase, Y., Tamai, S., Inoue, Y. & Shiro, M. (1992*a*). *J. Org. Chem.* **57**, 4238–4242.
Nagao, Y., Kumagai, T., Nagase, Y., Tamai, S., Inoue, Y. & Shiro, M. (1992*b*). *J. Org. Chem.* **57**, 4232–4237.
Nagao, Y., Nagase, Y., Kumagai, T., Kuramoto, Y., Kobayashi, S., Inoue, Y., Taga, T. & Ikeda, H. (1992). *J. Org. Chem.* **57**, 4238–4242.
Nagao, Y., Nagase, Y., Kumagai, T., Matsunaga, H., Abe, T., Shimada, O., Hayashi, T. & Inoue, Y. (1992). *J. Org. Chem.* **57**, 4243–4249.
Navas, J. J., Alemán, C., López-Carrasquero, F. & Muñoz-Guerra, S. (1997). *Polymer*, **38**, 3477–3484.
Ramachandran, K. I., Deepa, G. & Namboori, K. (2008). *Computational Chemistry and Molecular Modeling Principles and Applications*. Berlin: Springer.
Ramírez, R., Morillo, M., Arnal, M. L., López-Carrasquero, F., Martínez de Ilarduya, A. & Muñoz-Guerra, S. (2000). *Polymer*, **41**, 8475–8486.
Rietveld, H. M. (1969). *J. Appl. Cryst.* **2**, 65–71.
Robinson, R. P. & Donahue, K. M. (1992). *J. Org. Chem.* **57**, 7309–7314.
Schmidt, M. W., Baldridge, K. K., Boatz, J. A., Elbert, S. T., Gordon, M. S., Jensen, J. H., Koseki, S., Matsunaga, N., Nguyen, K. A., Su, S., Windus, T. L., Dupuis, M. & Montgomery, J. A. (1993). *J. Comput. Chem.* **14**, 1347–1363; http://www.msg.ameslab.gov/GAMESS/GAMESS.html.
Sheldrick, G. M. (2008). *Acta Cryst.* A**64**, 112–122.
Smith, G. S. & Snyder, R. L. (1979). *J. Appl. Cryst.* **12**, 60–65.
Spek, A. L. (2009). *Acta Cryst.* D**65**, 148–155.
Stephens, P. W. (1999). *J. Appl. Cryst.* **32**, 281–289.
Tanaka, K., Takenaka, H. & Caira, M. R. (2006). *Tetrahedron Asymm.* **17**, 2216–2219.
Thompson, P., Cox, D. E. & Hastings, J. B. (1987). *J. Appl. Cryst.* **20**, 79–83.
Toda, F., Tanaka, K., Yagi, M., Stein, Z. & Goldberg, I. (1990). *J. Chem. Soc. Perkin Trans 1*, pp. 1215–1216.
Wolff, P. M. de (1968). *J. Appl. Cryst.* **1**, 108–113.
Yang, Q.-C., Seiler, P. & Dunitz, J. D. (1987). *Acta Cryst.* C**43**, 565–567.